Anal. Bioanal. Electrochem., Vol. 16, No. 1, 2024, 79-99
https://www.doi.org/10.22034/abec.2024.710596

Analytical & Bioanalytical Electrochemistry

Full Paper

Bio- Electro-Fenton Process: Application to the Antiviral Ribavirin Mineralization in Aqueous Medium

I. Haji,[1] M. Shueai Yahya,[2] L. Rachidi,[1] I. Warad,[3] A. Zarrouk,[1,*] A. Talidi,[4] M. El Karbane,[5] and G. Kaichouh[1,*]

[1]*Laboratory of Materials, Nanotechnology and Environment, Faculty of Sciences, Mohammed V University in Rabat, P.O. Box. 1014, Rabat, Morocco*
[2]*Department of Chemistry, Faculty of Education, University of Hodeidah, Hodeidah, Yemen*
[3]*Department of Chemistry, AN-Najah National University, P.O. Box 7, Nablus, Palestine*
[4]*Laboratory for the Study of Advanced Materials and Application, Faculty of Sciences of Meknes, Higher School of Technology of Meknes, Moulay Ismail University of Meknes, Morocco*
[5]*Laboratory of Analytical Chemistry and Bromatology, Faculty of Medicine and Pharmacy of Rabat, University Mohammed V, Rabat, Morocco*

*Corresponding Author, Tel.: +212665201397 (A. Zarrouk); +212672210404 (G. Kaichouh)
E-Maisl: azarrouk@gmail.com (A. Zarrouk); g.kaichouh@gmail.com (G. Kaichouh)

Received: 17 November 2023 / Received in revised form: 1 January 2024 / Accepted: 23 January 2024 / Published online: 31 January 2024

Abstract- This work focuses on applying a combined process combining electro-Fenton (EF) pretreatment with biological degradation to mineralize the antiviral Ribavirin in an efficient, economical and ecological manner. First, the main experimental parameters affecting the efficiency of the electro-Fenton process, namely applied current intensity, Fe(II) catalyst concentration and initial Ribavirin concentration were evaluated and optimized. Indeed, the mineralization rate reaches maximum residual values of 99% after 4 hours of electrolysis applying a current of 200 mA. This mineralization is accompanied by an increase in biodegradability, evaluated from the BOD_5/COD ratio, which goes from 0.04 at the beginning of treatment (1 h) to 0.45 after 2 hours of electrolysis, demonstrating the feasibility of a biological treatment. In addition, the energy efficiency decreased when the treatment time was extended due to the limitation of mass transport. Thus, the feasibility of coupling electro-Fenton and biological treatment has been successfully demonstrated on a laboratory-scale was, achieving a 96.66% removal rate by the Bio-EF process. A Box-Behnken design based on response surface methodology was applied to develop a model for predicting Rib removal rate. The interaction of factors such as Rib concentration (X_1), catalyst concentration (X_2) and electrolysis time (X_3) was analyzed to identify optimal operating conditions. The model results

obtained are statistically significant with an R^2 of 0.99, indicating that the proposed model is significant and relevant. In addition, the iso-response curves obtained enabled us to determine the optimal experimental conditions required for effective mineralization of the targeted antiviral.

Keywords- Environmental pollution; Ribavirin; Electro-Fenton; Bio-Electro-Fenton; Biodegradability

1. INTRODUCTION

The increasingly worrisome environmental risk associated with the presence of pharmaceutical residues in wastewater is well known as a major concern worldwide, mainly related to their relative stability, meaning their difficult biodegradation and incomplete uptake by both animals and humans during their use [1], They are therefore molecules used for their intrinsic biological activities [2], they have the ability to cross cell membranes and remain as active molecules when excreted into the environment. In addition, their continued exposure even at low doses as well as potential toxicological effects on non-target organisms remains a problem for the scientific community [3]. Among the various emerging classes of pharmaceuticals are antiviral drugs that are used for treating certain viral infections, particularly influenza, herpes, hepatitis, and VIH [4].

Ribavirin (Rib) has been used for decades as an antiviral agent [5]. It is a synthetic, broad-spectrum nucleoside analog of guanosine that has shown activity against various DNA and RNA viruses [6,7]. Similarity of this compound to nucleosides explains this antiviral activity. Additionally, Ribavirin's clinical efficacy has been approved for treating a variety of viruses, namely influenza A and B viruses, respiratory syncytial virus (RSV) and parainfluenza and Lassa fever virus infections, also against HCV in combination with α-interferon [8–11]. Additionally, Ribavirin treatment may have some benefit against COVID-19 [12,13]. In fact, Rib has been widely used during this COVID-19 epidemic, resulting in a substantial increase in its concentration in wastewater effluents, especially in wastewater from pharmaceutical plants and hospitals. Continued release of large quantities of antiviral drugs and their metabolites into aquatic systems would cause the emergence of drug-resistant viral strains in wildlife, and viruses in their organisms could become resistant through rapid mutation [14]. And to limit this problem, studies have shown that these persistent organic residues and their degradation products can only be completely removed with advanced oxidation processes (AOPs) [15–17]. These processes have replaced traditional processes as simple and environmentally friendly techniques for treating various of persistent organic pollutants POPs [18]. Generally, these processes generate, in situ, hydroxyl radicals $^{\cdot}OH$, which have the highest oxidative power compared to classical oxidants H_2O_2, Cl_2, ClO_2^- or O_3 [19], and which react non-selectively with organic compounds until their mineralization (transformation of the pollutant into CO_2, H_2O and inorganic ions) [20–22].

The most studied and effective advanced oxidation process for treating persistent pollutants is the Electro-Fenton process, which combines the Fenton reaction with electrochemistry. This process relies on the in situ production of hydroxyl radicals ·OH from the Fenton reaction (Eq. (1)) in an acid media, where the Fe^{2+} regenerated by the electro-reduction of Fe^{3+} (Eq. (2)) generated by the Fenton reaction is combined with the in situ H_2O_2 generated by the reduction of the 2 electrons of dissolved oxygen O_2 (Eq. (3)) [23–27]. The EF process can be considered an environmentally friendly process because electricity is a clean energy source and does not produce secondary pollutants [28] and also achieves high degradation rates by converting bio-refractory molecules into biodegradable small molecules [29]. Indeed, this operation requires longer electrolysis times, which implies an important consumption of electrical energy, and consequently increase the global process costs [30,31]. On the other hand, eco-friendly bio-treatment options require carefully maintained reaction conditions and cannot always achieve satisfactory results in terms of removing toxic or microorganism-resistant organics [32].

$$Fe^{2+} + H_2O_2 \rightarrow Fe^{3+} + {}^{\bullet}OH + OH^- \quad (1)$$

$$Fe^{3+} + e^- \rightarrow Fe^{2+} \qquad E^\circ = 0,77\ V/\ ESH \quad (2)$$

$$O_2 + 2H^+ + 2e^- \rightarrow H_2O_2 \qquad E^\circ = 0,69\ V/\ ESH \quad (3)$$

Taking into account the advantages and disadvantages of both electrochemical oxidation and biological treatment, combining both processes is considered a suitable solution, reducing operating costs and obtaining a profitable technique [33,34]. In the combined process, electrochemical oxidation has been used as a pretreatment step for converting persistent organic pollutants POPs to biodegradable and less toxic intermediates, which could be easily removed in a subsequent activated sludge bio-oxidation step, thus saving energy and lowering the overall cost of treatment [35,36]. On the other hand, the EF process is highly dependent on different operating conditions that necessitate developing an experimental model allowing the study and optimization of their influence during the electrochemical process.

Response surface methodology represents a commonly applied mathematical and statistical tool to assess independent parameters (variables) effects on response [37,38]. Indeed, this methodology allows the experiments design, the construction and analysis of models, the evaluation of the effects of factors, and thus the search for the optimal conditions to obtain the desired response [39], and even in the presence of complex interactions, it can solve multivariate equations and evaluate the relative importance of several influencing factors. Indeed, this methodology allows the experiments design, the construction and analysis of models, the evaluation of the effects of factors, as well as the search for optimal conditions to obtain the desired response [39], and even in the presence of complex interactions, it can solve multivariable equations and evaluate the relative importance of several influencing factors [40]. It is also a simple, effective way to obtain maximum information with a minimum of experimental tests [41–43]. RSM contains several advantageous methods in which the Box-

Behnken design is numerically applied due to its low cost in time (reduced number of trials) and resources invested in experiments. Indeed, this design involves fewer trials, allows the response function to be estimated at intermediate levels and is more efficient than other RSM designs [44]. The Box-Behnken design BBD has many applications in several scientific fields. It has been used to optimize several chemical and physical processes through its rational design and good results [39].

2. EXPERIMENTAL SECTION

2.1. Chemicals

In this study, we used different chemical reagents, of analytical quality and without prior purification. Ribavirin "Rib" (Figure 1) with chemical formula $C_8H_{12}N_4O_5$, is an odorless tablet, with solubility in water, ethanol, and dimethyl sulfoxide, and low solubility in alcohol [10] was obtained from Sigma-Aldrich. Ferrous sulfate $FeSO_4.7H_2O$ (catalyst source, 99%), sodium sulfate (Na_2SO_4), potassium chloride KCl, and sulfuric acid H_2SO_4 (purity 96%), were obtained from Shanghai chemicals (Shanghai, China). In addition, preparation of all aqueous solutions was done using ultrapure water, obtained from a Millipore Milli-Q system.

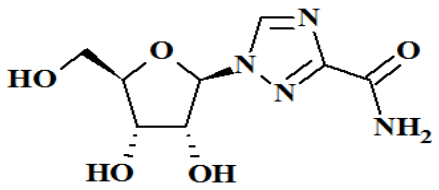

Figure 1. Ribavirin chemical structure

2.2. Electrolytic system

The electrochemical mineralization process of the Rib antiviral was carried out in an electrochemical cell with three electrodes at ambient temperature. A platinum (Pt) anode (2.5 cm × 2 cm) vertically placed at the cell center and a three-dimensional carbon felt cathode (6 cm × 5 cm × 0.5 cm) placed inside the cell wall. In a compartment separated from the other two electrodes by sintered glass, the reference electrode is placed, which is a saturated calomel electrode KCl. The Potentiostat/Galvanostat type PGZ301 Voltalab instrument was used to impose the current applied between the electrodes. An amount of Rib was introduced in the electrochemical cell adding iron sulfate heptahydrate $FeSO_4.7H_2O$ as a source of catalyst with an amount of sodium sulfate (0.05 M) as a support electrolyte to ensure the conductivity of the reaction medium. In addition, compressed air was bubbled for 10 minutes before the start of each electrolysis to saturate the solution with oxygen. Solutions were fixed at pH 3 by adding sulfuric acid H_2SO_4. The solutions were kept under constant magnetic stirring to ensure mass transfer to the electrodes.

2.3. Aerobic biological treatment

Duplicate cultures were performed within Erlenmeyer flasks holding 200 mL of Ribavirin solution (0.3 mM) that was non-electrolyzed and pre-electrolyzed by the electro-Fenton process, closed with Cotton plug to ensure oxygenation. Minerals and trace elements were introduced into the culture medium [45]; The solution has been adjusted to pH 7 by NaOH. Activated sludge from a local wastewater treatment plant (Ain El Ouda) was added at an initial concentration of 1 $g.L^{-1}$ in dry matter. Cultures were agitated at ambient temperature and 5 mL samples were periodically taken, filtered and injected for COD measurements.

2.4. Analysis methods

Chemical oxygen demand (COD) of both initial and treated samples was measured by dichromate method using a DR/125 spectrophotometer (Hach Company USA). In order to perform the method, a sufficient quantity of sample is introduced into a mixture containing Potassium Dichromate $K_2Cr_2O_7$, Sulfuric Acid H_2SO_4 and Mercury Sulfate $HgSO_4$. The mixed solution was then incubated at 150 °C for 120 min.

The Instantaneous current efficiency (ICE**)** has been determined according to formula (4) [46,47]. Where, COD_o and COD_t are referring respectively to COD initial and final values, I is a current applied (A), F is Faraday's constant (96 487 C mol^{-1}), V is the volume of solution (L) and t is the processing time (s), 8 is the dimensionality factor for unit consistency [(32 g of $O_2.M^{-1}$) / (4 mol of electron exchanged)].

$$ICE = \frac{(COD_0 - COD_t)F.V}{8.I.t} \quad (4)$$

Energy consumption (EC) constitutes one major parameter for estimating an electrochemical process's operational cost. It is usually expressed in kWh consumed per kg of COD removed, according to the following equation (5) [46–48]. Where, E_{cell} is the cell average voltage (V), t is time of electrolysis (h), I is the current applied (A), $(\Delta COD)_t$ COD decrease (g L^{-1}) at time t and Vs is the solution volume (L).

$$EC = \frac{E_{cell}.I.t}{(\Delta COD_t).V_s} \quad (5)$$

Biological oxygen demand (BOD) indicates oxygen necessary for aerobic microorganisms to oxidize dissolved or suspended organic matter. It is measured after 5 days at 20 °C (temperature favorable to the activity of O_2 consuming microorganisms) and in darkness in order to prevent any parasitic photosynthesis. A pH of 6.5- 7.5 was adjusted and the N-allylthiourea was added as a nitrification inhibitor, KOH pellets were introduced into the flasks to trap CO_2. The Ribavirin molecule was biologically degraded using municipal wastewater obtained from the National Office of Electricity and Drinking Water, Rabat, Morocco.

2.5. Experimental design (Box-Behnken Design)

In the present study, the RSM has been implemented using the Box-Behnken design to optimize the electrochemical mineralization process of the antiviral Ribavirin. This design was chosen because of its easy implementation, as all factors take only three levels: - 1, 0, and + 1, in coded variables [38,42]. It includes twelve trials to which one or more center points can be added. Both data design and statistical analysis were performed using the Design Expert software. The latter was used to evaluate, the influence of three independent factors, namely the pollutant concentration [Rib] (X_1), the catalyst concentration [Fe^{2+}] (X_2) and the time of electrolysis (X_3), on the COD removal rate (%), while setting the solution pH to 3 and the current intensity I to 200 mA. Each chosen factor was examined in three levels, one level, low (-1), medium (0) and high (+1) (Table 1), representing 15 total experiments with three central point replications. In order to express the relationship existing among the process independent variables and the predicted response Y (COD removal rate (%)), a second degree polynomial equation was fitted (Eq. (6)), where β_0 is the constant term, β_i is the linear coefficient, β_{ii} is the quadratic coefficient, and β_{ij} is the interaction coefficient.

$$Y = \beta_0 + \sum_{i=1}^{k} \beta_i X_i + \sum_{i=1}^{k} \beta_i X_i^2 + \sum_{i_{j=1}}^{k} \sum_{j>1}^{k} \beta_{ij} X_i X_j \qquad (6)$$

The model was statistically analyzed using ANOVA to investigate interaction among the three independent factors influencing COD removal rate (%) (Response). The latter can be calculated using equation (7) where COD_0 and COD_t represent COD initial and final values [49, 50].

$$CODremoval(\%) = \frac{COD_0 - COD_t}{COD_0} \times 100 \qquad (7)$$

Table 1. Coded and actual values for optimizing the EF process via the Box-Behnken design

Factor	Variables	Coded and actual values		
		-1	0	+1
X_1	$[RIB]_0$ (mM)	0.1	0.2	0.3
X_2	$[Fe^{2+}]_0$ (mM)	0.05	0.1	0.15
X_3	$t_{electro}$ (hour)	1	2	3

Polynomial quadratic model performance was assessed by the correlation coefficient 'R^2', and it was tested for statistical significance by Fisher's F test. Thus, identifying the experimental parameters that have a statistically significant effect on the response was done using p-values. If these are below 0.05, the response is statistically significant at the 95% confidence level.

3. RESULTS AND DISCUSSION

3.1. Effect of the parameters influencing the Ribavirin mineralization

3.1.1. Applied current effect

It's generally proven that the applied current density significantly affects the electrochemical oxidation of organic compounds since the hydroxyl radicals quantity generated depends on the current intensity applied [51–53]. The applied current effect on the mineralization of 0.3 mM Rib in the presence of 0.1 mM ferrous ion was presented in Figure 2.The latter shows that increasing the current density favors hydroxyl radical formation and consequently leads to a higher Rib mineralization efficiency (Figure 2(a)). Indeed, a 99% COD removal was achieved applying a 200 mA current during 4 hours of electrolysis. This enhancement in removal rate may be ascribed to increased electrochemical reaction rate resulting in faster production of Fenton reagents (Fe^{2+} and H_2O_2) and consequently, a significant amount of hydroxyl radicals. On the other hand, it is observed that for a high value of the applied current (I= 300 mA), the Rib mineralization rate becomes slow. It is possible to explain this behavior by the overconsumption of electrical energy by parasitic reactions susceptible to occur at increased current intensities: notably the electrochemical O_2 reduction (with exchange of 4 e-) leading to the H_2O formation (Eq. (8)), the increasing H_2 formation at cathode (Eq. (9)) and H_2O_2 oxidation at anode (Eq. (10)) [23,36,54].

$$O_2 + 4e^- + 4H^+ \rightarrow 2H_2O \quad (8)$$

$$2H_2O + 2e^- \rightarrow H_2 + 2OH^- \quad (9)$$

$$H_2O_2 \rightarrow O_2 + 2H^+ + 2e^- \quad (10)$$

In order to quantify the effect of applied current on the electrochemical mineralization of Rib, the instantaneous current efficiency (ICE) was determined using equation 4. The calculation results (Figure 2(b)) show that the best ICE% values are obtained at low electrolysis currents. It should also be noted that the ICE% decreases with increasing applied current density, down to 300 mA. This decrease can mainly be associated with aromatic compounds disappearing in the media and forming short-chain carboxylic acids, which resist mineralization and promote undesirable reactions [55]. Furthermore, during these experimental conditions (high current and long electrolysis time), two parasitic reactions (Eq. (9,11)) become dominant [56], which could interfere with the Fenton reagent generation.

$$Fe^{2+} + {}^{\bullet}OH \rightarrow Fe^{3+} + OH^{-} \quad (11)$$

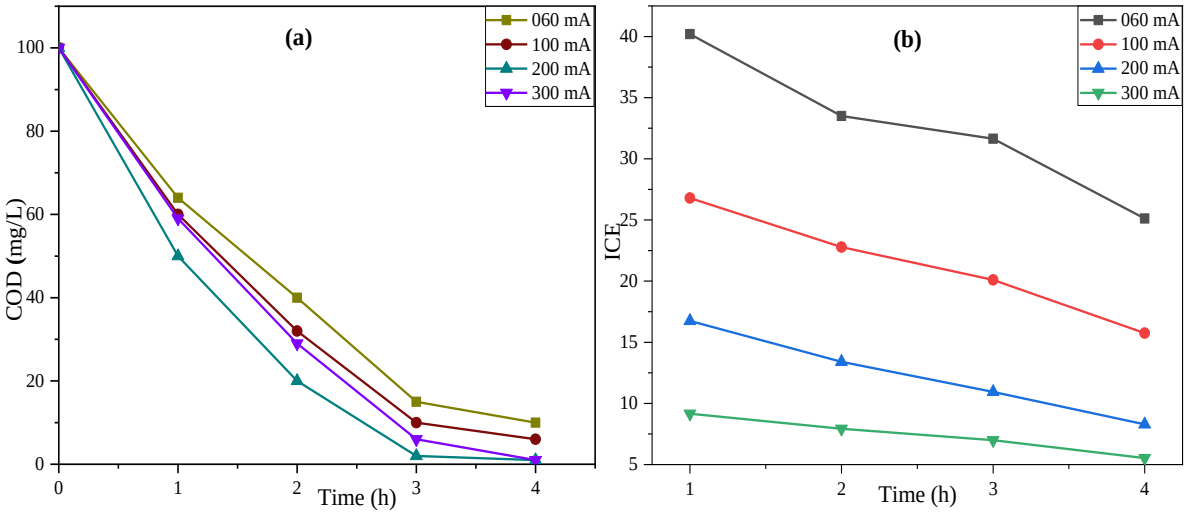

Figure 2. Applied current effect on: (a) Mineralization, (b) Instantaneous current efficiency ICE, during Ribavirin treatment by Electro-Fenton process (EF); $[Rib]_0$ = 0.3 mM; $[Fe^{2+}]$ = 0.1 mM; $[Na_2SO_4]$ = 0.05 M; V = 0.2 L; pH = 3

3.1.2. Effect of Fe(II) catalyst concentration

Ferrous ions addition to the solutions also affects the EF process efficiency to remove persistent organic pollutants POPs [46]. They may react with H_2O_2 formed on the cathode surface to generate hydroxyl radicals ·OH [57]. Hence, experiments were performed by varying the initial Fe^{2+} concentration from 0.05 to 0.2 mM, with an applied current of 200 mA, in order to evaluate the effect of the initial catalyst concentration on the mineralization process of the targeted antiviral agent (Figure 3).

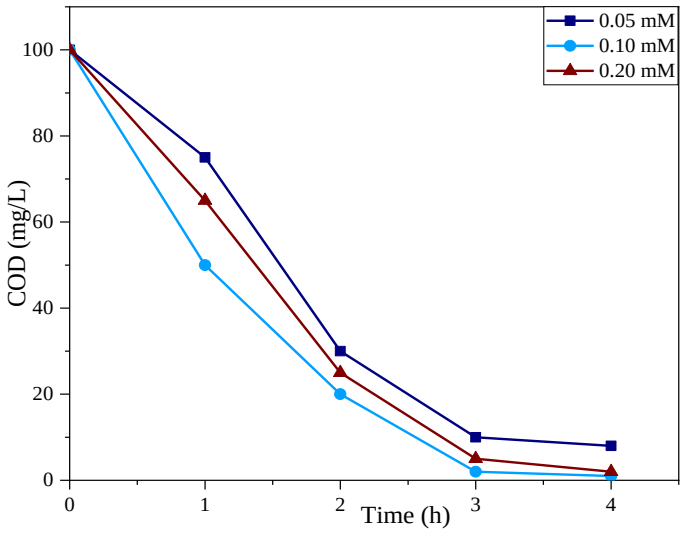

Figure 3. Catalyst concentration effect on the Ribavirin mineralization by the EF process. $[Rib]_0$ = 0.3 mM; $[Na_2SO_4]$ = 0.05 M; V = 0.2 L; pH = 3; I = 200 mA

As can be seen, at a catalyst concentration of 0.05 mM, the mineralization rate is slow and then slightly increases as the Fe^{2+} concentration increases from 0.05 to 0.1 mM. Conversely, increasing in catalyst concentration above 0.1 mM resulted in decreased mineralization efficiency. This phenomenon seems to be attributed to the increasing rate of parasitic reaction between ·OH and Fe^{2+} according to equation (11). Indeed, it is known in the literature that at high Fe^{2+} concentration, this reaction, which consumes hydroxyl radical's ·OH, is favored and comes into competition with hydroxyl radicals, which weakens the oxidation reaction of the studied antiviral [17,20,58].

3.1.3. Effect of the initial Ribavirin concentration

Generally, the initial pollutants concentration remains a major parameter in wastewater treatment [59]. The COD evolution under optimal pH and current conditions using different Rib concentrations: C_0= 0.1, 0.2, 0.3 mM was evaluated. Figure 4 shows that in all cases, the COD decreases with time. Moreover, it is noted that the electrolysis time required for mineralization is slower at higher initial concentration. This phenomenon could be associated with the aliphatic intermediates formation (especially carboxylic acids) before the complete solution mineralization in CO_2 and H_2O and inorganic ions, which have less reactivity toward the ·OH species, leading to a decrease in the mineralization rate [56]. In contrast, at a 0.1 mM Ribavirin concentration, COD rate was 99%. This result suggests that at increased Rib concentrations, some intermediates accumulate, resulting in decreased pollutant removal efficiency.

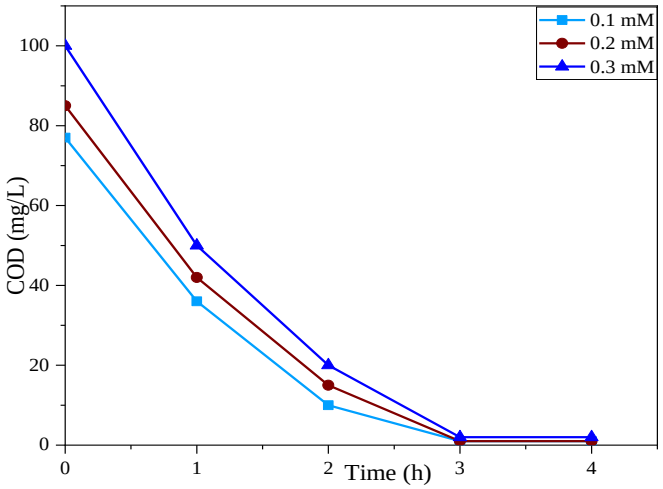

Figure 4. Initial Ribavirin concentrations effect on the COD evolution during EF treatment; [Fe^{2+}] = 0.1mM; [Na_2SO_4] = 0.05 M; V = 0.2 L; pH = 3; I = 200 mA

3.1.4. Energy consumption

Energy consumption (EC) proves to be an important parameter for providing a better insight into the operating cost of the electrochemical cell during the removal process and to

establish its sustainability on an industrial scale. Figure 5 shows the calculated EC results (from Equation 5) as a function of electrolysis time and at different current intensities. As can be seen, an increase in energy consumption depends directly on the applied current intensity and the treatment time (Figure 5). In fact, the lowest energy consumption was recorded at lower current intensity (100 mA), this is also confirmed by the low cell potential (E_{cell}) and higher ICE values. Similarly, the lowest energy expenditure was recorded for the lowest electrolysis times (1 h). In contrast, a higher current intensity for longer treatment times leads to similarly high energy consumption, which might be explained by increasing parasitic reactions, namely O_2 liberation at the anode and H_2 at the cathode as well as destroying H_2O_2 on both cathode and anode. Practically, complete mineralization is not required, as most toxic organic compounds (especially aromatic compounds) transform into small biodegradable molecules within the first two to three hours of treatment. In this regard, the implementation of a removal process combining an electrochemical process with a cost-effective biological process "Bio-Electro-Fenton" has proved a more energetically efficient means for treating recalcitrant contaminants [60].

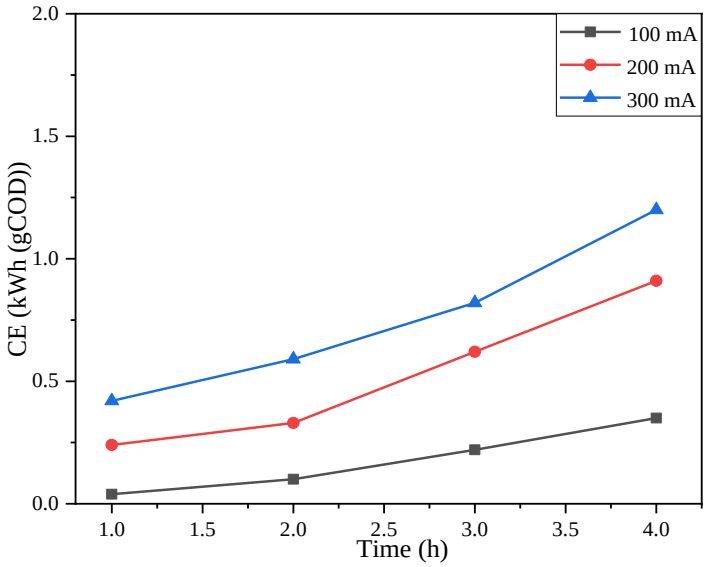

Figure 5. Evolution of the energy consumption E (kWh / (g COD)) during the EF process

3.2. Study of the Ribavirin biodegradability

Although AOPs have a strong ability to completely mineralize persistent organic pollutants, it is more beneficial to use them only to improve the biodegradability of these persistent substances prior to incorporating them into a biological treatment process [61]. The feasibility of the latter is verified by tests of solutions biodegradability. In fact, this parameter is defined through the BOD_5/COD ratio, regarded as an indicator of biodegraded organic matter. Generally, a 0.4 value is admitted as a biodegradable threshold beyond which a solution can be considered as easily biodegradable [31,62,63].

The evolution of the BOD_5/COD ratio during EF treatment under selected optimal conditions is presented in Figure 6. The results showed that Ribavirin was not biodegradable prior to electrolysis with a BOD_5/COD ratio of zero. After 1 hour of electrolysis, this ratio remains low (BOD_5/COD= 0.04). This indicates that the biodegradability of the by-products was poor during this period. However, after electrolysis for 120 min, a ratio of 0.45 was obtained, indicating that the treated solution was readily biodegradable. This may be caused by refractory by-products being oxidized by hydroxyl radicals and consequently a generation of biodegradable intermediates [64]. Furthermore, the biodegradability of the resulting electrolyzed solution decreased with increasing electrolysis time, with a BOD_5/COD ratio decreasing from 0.8 to 0.3 after 300 min, which is consistent with related literature, which may be associated with the recalcitrant quinolone cycle accumulation with increasing electrolysis time [65,66]. Therefore, pretreatment with EF for 2 hours further improves the biodegradability of the solution.

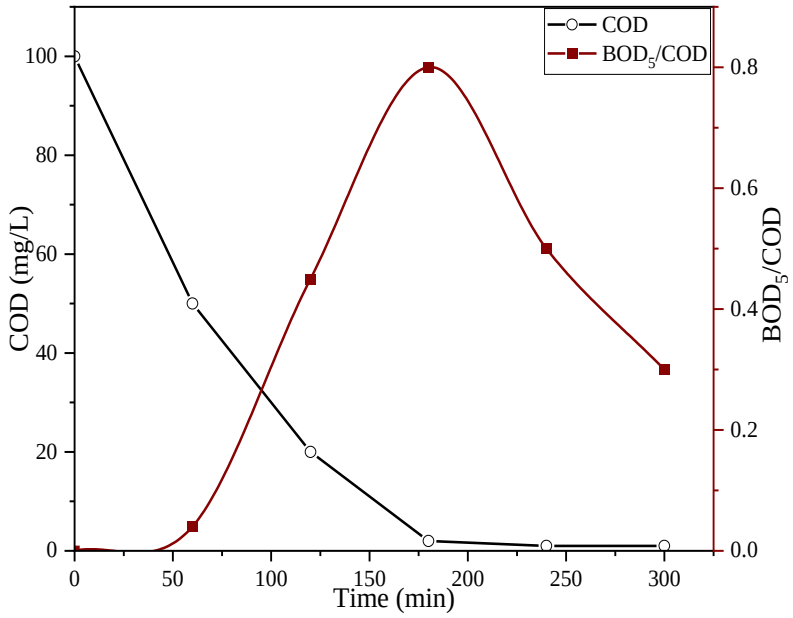

Figure 6. Biodegradability evolution (BOD_5/COD ratio) and mineralization during EF treatment at I = 200 mA; $[Rib]_0$=0.3 mM; $[Fe^{2+}]$ =0.1 mM; pH =3; $[Na_2SO_4]$=0.05 mM

3.3. Biological aerobic treatment

The estimation of the BOD_5/COD ratio during electrochemical treatment is extremely important to examine the interest of the pretreatment and to optimize subsequently the electrolysis time necessary to pass to the bio-treatment. Indeed, the biodegradability tests obtained allowed us to justify the choice of 2 hours to adapt the solution to a biological oxidation step. Indeed, after an electrochemical pretreatment of 2 hours, the solution was then treated biologically with activated sludge, in duplicate, in aerobic conditions for 20 days. The COD removal rate evolution during the combined process was illustrated in Figure 7(b). It can

be seen that after 4 days of cultivation the microorganisms were able to degrade up to 43% of the organic matter contained in the pretreated solution, indicating that the intermediates generated by the electrochemical process are slightly biocompatible (as the increase of the BOD_5/COD ratio suggests). In contrast, no biodegradation of the non-pretreated Rib was observed by the aerobic treatment (Figure 7(a)). In fact, the biosorption test of the Rib antiviral on activated sludge during the first two hours of the aerobic treatment, showed no change in the COD content, confirming the recalcitrance of the targeted antiviral, which is consistent with the low BOD_5/COD ratio. Generally, biosorption is regarded as a rapid phenomenon that could be observed during the first two hours of the experiment [67]. Finally, after 18 days, the overall efficiency of mineralization at the end of the activated sludge biological process was 96.66%, showing the high performance of the "Bio-EF" combined process compared to individual treatment options, harnessing EF's high oxidative capacity and its disadvantages (high cost) are offset by combining it with a low-cost, environmentally friendly biological method. Quite similar results with over 90% COD removal were obtained, demonstrating that the use of EF as a pretreatment proved to be more effective and economical [31].

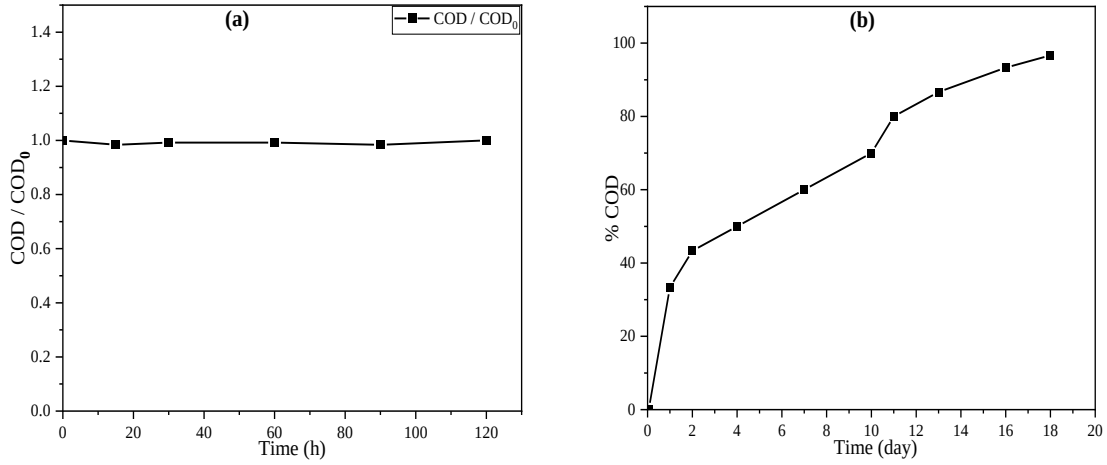

Figure 7. Mineralization evolution during activated sludge biological treatment at 25 °C; pH=7 of a Rib pretreated solution for 2 hours by EF at I=200 mA; $[Rib]_0$=0.3 mM; $[Fe^{2+}]$ =0.1 mM; pH =3; $[Na_2SO_4]$=0.05 mM

3.4. COD Removal Efficiency Optimization

3.4.1. Modelling and statistical analysis by the Box-Behnken Design (BBD)

In order to statistically analyze the main variables affecting aqueous removal of the antiviral Ribavirin by the Electro-Fenton process, a three-level Box-Behnken Design (BBD) was performed and response surface plots were drawn. On this basis, the second-degree polynomial equation given in coded variables (Eq. (12)), where X_1, X_2 and X_3, represent the values of pollutant concentration, Fe^{2+} catalyst concentration and electrolysis time, was fitted to the

experimental values (Table 2) obtained, with the aim of reducing a combined effects of the three independent variables.

$$COD removal(\%) = -48 + 593.75X_1 + 682.5X_2 + 10X_3 - 100X_1X_2 + 12.5X_1X_3 + 55X_2X_3 - 1400X_1^2 - 4000X_2^2 + 1.25X_3^2 \quad (12)$$

This equation indicates that regression is significant for all linear terms and the X^2_1 and X^2_2 quadratic coefficients, as well as the factorial interaction X_2X_3 was also significant. The X_1X_3 factorial interaction may be significant ($p \approx 0.0503$) but not so critical, whereas the quadratic effects of X^2_3 and the X_1X_2 factorial interactions had no significant effect on the treatment process ($p > 0.05$) (Table 3). Regression of the optimal polynomial model for COD% yield was performed only considering significant terms for which p-value was below 0.05 [42,68]. Coefficients having a positive sign indicate a synergistic effect, while those with a negative sign indicate an antagonistic effect [69].

Table 2. Box-Behnken design including experimental and predicted values of expressed response

Run	**Independent Variables**			**Response % COD**
	X_1 (mM) Cp Pollutant concentration	X_2 (mM) Catalyst concentration	X_3 (h) Electrolysis time	COD removal %
1	0.2	0.05	3	94
2	0.2	0.1	2	82
3	0.3	0.1	1	50
4	0.1	0.15	2	52
5	0.1	0.1	3	86
6	0.3	0.10	3	99
7	0.1	0.10	1	42
8	0.2	0.10	2	82
9	0.2	0.05	1	54
10	0.2	0.15	3	98
11	0.3	0.15	2	60
12	0.2	0.15	1	47
13	0.3	0.05	2	65
14	0.2	0.1	2	82
15	0.1	0.05	2	55

Table 3. ANOVA test for quadratic model

Source	Sum of Squares	df	Mean Square	F-value	p-value	
Model	5526.98	9	614.11	646.43	< 0.0001	Significant
A-[Rib]	190.13	1	190.13	200.13	< 0.0001	
B-[Fe^{2+}]	15.13	1	15.13	15.92	0.0104	
C-time	4232.00	1	4232.00	4454.74	< 0.0001	
AB	1.0000	1	1.0000	1.05	0.3520	
AC	6.25	1	6.25	6.58	0.0503	
BC	30.25	1	30.25	31.84	0.0024	
A^2	723.69	1	723.69	761.78	< 0.0001	
B^2	369.23	1	369.23	388.66	< 0.0001	
C^2	5.77	1	5.77	6.07	0.0569	
Residual	4.75	5	0.9500			
Lack of Fit	4.75	3	1.58			
Pure Error	0.0000	2	0.0000			
Cor Total	5531.73	14				

Table 4. ANOVA statistical parameters of the regression model

Variable	
R^2	0.9991
Adjusted R^2	0.9976
Predicted R^2	0.9863
C.V. %	1.40
Adeq. precision	70.0533

The tests of analysis of variance (ANOVA) were also carried out to evaluate both validity and significance of the proposed mathematical model (Table 4). Model fit was assessed using the correlation coefficient. Indeed, the model predicted response is accurate if the R^2 value is close to unity (1) [70]. In our case, the model correlation coefficient (R^2 = 0.999) as well as fitted correlation coefficient (Adj.R^2 = 0.997) are very close to the ideal value of 1, and are not significantly different from each other, indicating the excellent correlation existing between observed and predicted values, thus confirming that the proposed model is important and

relevant. In addition, the model p-value was well below the 0.05 significance level, indicating model significance. Furthermore, the large F-value for no fit indicates significance of no fit and accuracy of the obtained models. Generally, a higher F-value and a lower P-value indicate that the expression of the corresponding coefficient is more significant [71].

The coefficient of variation (CV) allows describing the range of data variation and it's also used to measure reproducibility. A value less than 10% is acceptable for the proposed model to be reproducible [72,73]. In this study, a coefficient of variation of 1.40% was obtained, confirming the reproducibility of the COD removal model. Adequate accuracy to measure the signal-to-noise ratio was also evaluated. Indeed, a ration greater than 4 is required to consider the model satisfactory [74]. The COD removal model yields a ratio of 70.05 indicating that the signal from the model is adequate and that the model may be applied to route the concept space.

A normality test was performed to verify the model quality and whether the actual data follow a normal distribution or not. The normal probability linear plot against the adjusted values for the removal efficiency of COD (Figure 8) confirms that the model follows a normal distribution, i.e. a satisfactory accord between experimental and predicted data exists, due to the very close proximity of the experimental data to the straight line.

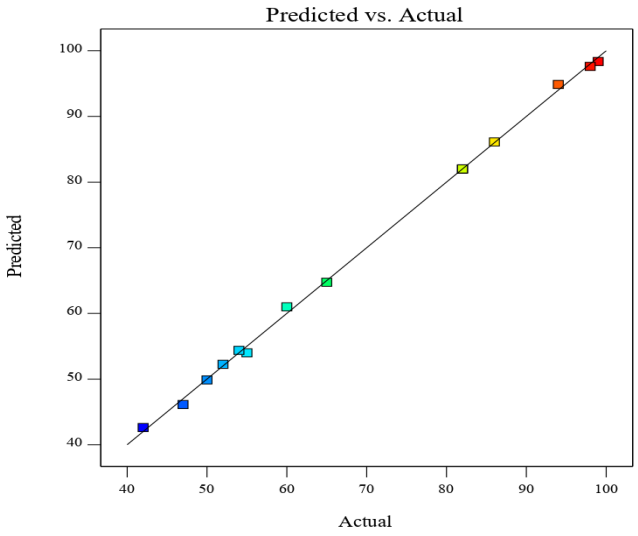

Figure 8. Normal probability plot

The response surface plots of the independent parameters affecting the COD removal rate by the EF process are presented in Figure 9. These plots were made varying two process variables, while keeping the pH fixed at 3 (ideal pH for the proper operation of the EF process [75]), applying a current of 200 mA, in order to visualize the parameters interaction effect on the COD removal rate. Indeed, the interaction of Fe^{2+} catalyst concentration and the electrolysis time (Figure 9(a)) shows that the increased electrolysis time generally favors the COD removal rate. Indeed, a 99% removal rate was recorded for an electrolysis time of 3 hours. Moreover, the removal rate of the Rib antiviral reached its maximum for a catalyst concentration in the

domain middle (0.1 mM). On the other hand, for concentrations above 0.1 mM, the system efficiency decreases as a result of increasing rates of parasitic reactions, consuming the hydroxyl radicals and inhibit the Fenton reaction by consuming its reactants (Eq. 11) [25]. However, there is an obvious interaction between Fe^{2+} catalyst concentration (X_2) and electrolysis time (X_3) for Rib antiviral removal (X_2X_3 for p= 0.0024), as shown in tab. 3. Furthermore, the interaction between initial Rib concentration and electrolysis time (Figure 9(b)) shows that there is an influence on the COD removal rate, with a significant X_1X_3 coefficient (p-value at the significance level p= 0.0503). However, the interactions effect of the initial Rib concentration (X_1) and catalyst concentration (X_2) (Figure 9(c)) is insignificant (X_1X_2 for p= 0.3520).

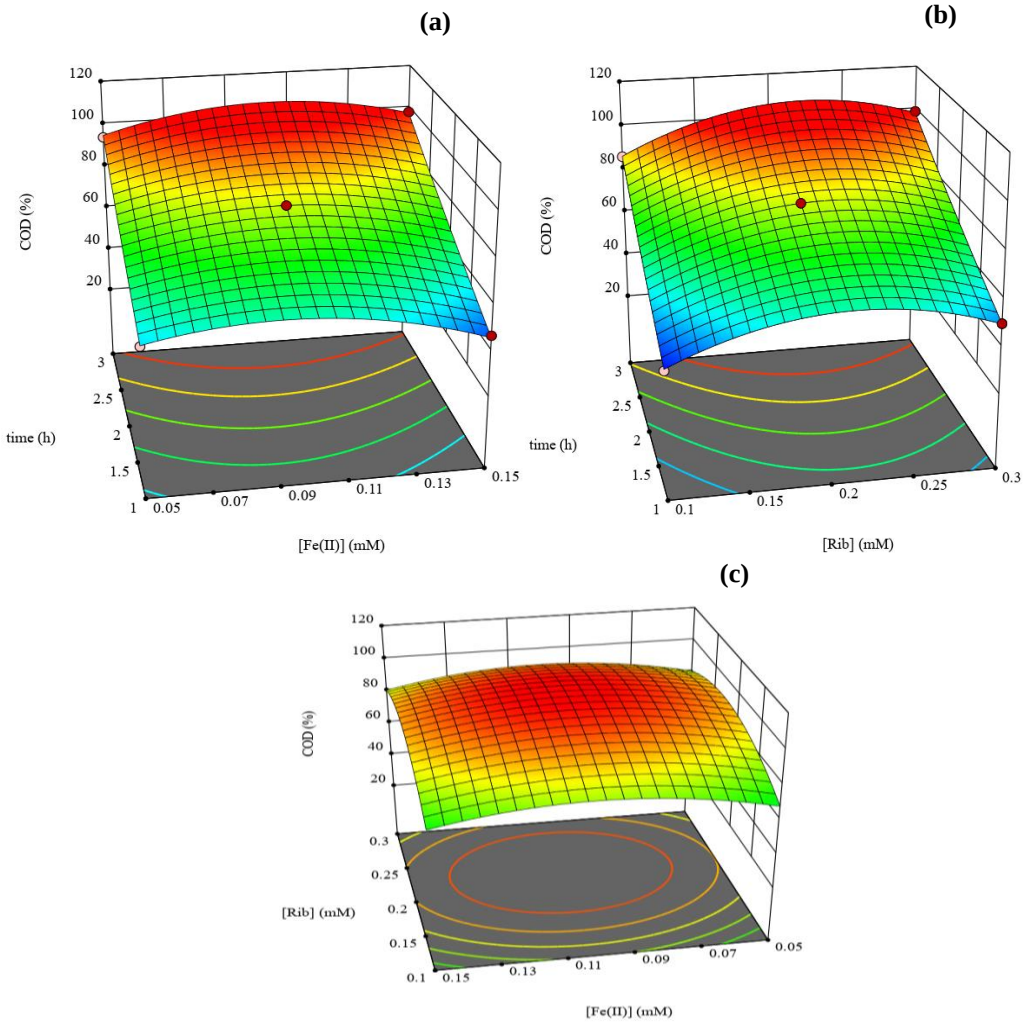

Figure 9. Three-dimensional surface response plots of COD removal from Rib by the EF process

3.4.2. Process Optimization

After the modeling phase which allows developing a second order model and which reflects in a reliable way the variation effect in the various functioning parameters in particular, the

electrolysis time, initial concentration of the catalyst and the initial concentration of the Rib, on the COD removal rate, we are engaged in the optimization step which consists in determining the values of the parameters leading to maximum COD removal rates (Table 5). In fact, an almost total mineralization of 99.92% was achieved during 3 hours of electrolysis with a catalyst concentration very close to 0.1 mM, which was confirmed through empirical experiments under similar conditions. In several studies, using RSM has been shown to be effective in optimizing a proposed model and determining the optimal parameters [72].

Table 5. Optimal operating conditions for the EF process

[Rib] (mM)	**[Fe^{2+}] (mM)**	**Time (h)**	**COD Removal**	**Desirability**
0.230	0.095	2.736	99.929	1.000

Studies have also examined the effect of three independent factors on the electrochemical removal efficiency of organic micro pollutants by the Electro-Fenton process using Box-Behnken design (BBD) based statistical response surface methodology (RSM) at three levels (Table 6). The latter clearly shows that BBD based RSM was a powerful and easy technique for optimizing EF process operating conditions to effectively remove emerging pollutants from aqueous media.

Table 6. Electro-Fenton process optimization for organic micro pollutant treatment using the Box-Behnken concept

Micropollutant	**Optimum conditions**	**R^2**	**Removal efficiency**	**Ref.**
Phenol	[Fe^{2+}]= 0.1 mM, $t_{electro}$= 5 h I= 4.237 mA/cm2	0.9803	81.335 %	[76]
Mix of Fluoroquinolones (FQs)	[Fe^{2+}] = 0.31 mM; $[FQs]_0$ = 87.0 mg L^{-1} I = 244.0 mA cm×2.	0.5710	61.12 %	[77]
Tenofovir (TEN)	I= 282 mA [TEN]= 0.1 mM $t_{electro}$= 164 minutes	0.9748%	98%	[78]

4. CONCLUSION

The mineralization of the antiviral Ribavirin by the electrochemical oxidation process "Electro Fenton" alone and combined with biological treatment was examined. An almost

complete Rib mineralization was obtained after 4 hours of electrolysis applying a current intensity of 200 mA with a 0.1 mM catalyst (Fe(II)) concentration, thus achieving an optimum Ribavirin concentration of 0.3 mM. Biodegradation tests of Ribavirin from treated and untreated solutions by the EF process under the optimal conditions showed that at the beginning of the electrolysis, Ribavirin was not biodegradable with a $BOD_5/COD= 0$ ratio. However, a $BOD_5/COD= 0.45$ ratio was achieved after 2 hours of electrolysis, indicating that the initially non-biodegradable and toxic drug solution is converted to a biodegradable solution. Furthermore, after 18 days of biological treatment, the overall COD removal rate increased significantly, up to 96.66 % for the Rib solution pretreated electrolyzed for 2 hours. This proves the suitability of the combined process for treating non-biodegradable organic compounds. The modeling and optimization of the operating conditions affecting the process of Rib removal by Electro-Fenton were performed by applying the response surface methodology according to the Box-Behnken design. Indeed, the model obtained is statistically significant with an R^2 of 0.99. Moreover, the study of the iso-response curves obtained allowed us to determine the optimal experimental conditions necessary for the efficient mineralization of the targeted antiviral.

Declarations of interest

The authors declare no conflict of interest in this reported work.

REFERENCES

[1] T. Rasheed, M. Bilal, F. Nabeel, M. Adeel, and M.N. Iqbal. Environ. Int. 122 (2019) 52.
[2] A. Ginebreda, I. Muñoz, M. López, D. Alda, R. Brix, J. López-doval, and D. Barceló, Environ. Int. 36 (2010) 153.
[3] J.P. Fernandes, C.M.R. Almeida, M.A. Salgado, M.F. Carvalho, and A.P. Mucha, Toxics 9 (2021) 257.
[4] C. Nannou, A. Ofrydopoulou, E. Evgenidou, E. Heath, and D. Lambropoulou, Sci. Total Environ. (2019) 134322.
[5] E. Thomas, M.G. Ghany, annd T.J. Liang, Antivir. Chem. Chemother. 23 (2012) 1.
[6] A.A. Youssef, N. Magdy, L.A. Hussein, J. Chromatogr. Sci. (2019) 1.
[7] E. Zironi, T. Gazzotti, B. Lugoboni, A. Barbarossa, A. Scagliarini, and G. Pagliuca, J. Pharm Biomed. Anal. 54 (2011) 889.
[8] Z. Xu, Y. Ji, M. Guan, H. Huang, C. Zhao, and H. Zhang. Appl Surf Sci. 256 (2010) 3160.
[9] IA. Darwish, HF. Askal, AS. Khedr, and R.M. Mahmoud, J. Chromatogr. Sci. 46 (2008) 4.
[10] G.R. Babu, A.L. Rao, and J.V. Rao. Int. J. Pharm. Pharm. Sci. 7 (2015) 2.
[11] F. Belal, M.K.S. El-din, M.I. Eid, and R.M. El-gamal. J. Chromatogr. Sci. (2014) 1.

[12] H. Zhu, N. Sze, A. Mak, Y. Yan, and Y. Zhu. J. Med. Virol. (2020) 740.
[13] Y. Xu, M. Li, L. Zhou, D. Liu, W. He, W. Liang, Q. Sun, H. Sun, Y. Li, and X. Liu. Infect Drug Resist. 14 (2021) 5287.
[14] S. Lei, X. Chen, J. Wu, X. Duan, and K. Men, Sig Transduct Target Ther. 7 (2022) 387.
[15] F. Zaviska, P. Drogui, G. Mercier, and J.F. Blais. Rev. des Sci. 22 (2009) 535.
[16] N. Oturan, M. Panizza, and M.A. Oturan. J. Phys. Chem. A 113 (2009) 10988.
[17] H. He, and Z. Zhou. Crit. Rev. Environ. Sci. Technol. 47 (2017) 2100.
[18] M. Arellano, N. Oturan, M. Pazos, M. Ángeles Sanromán, and M.A. Oturan. Sep. Purif. Technol. 233 (2020) 115990.
[19] De Dios MÁ. Fernández, O. Iglesias, M. Pazos, and M.Á. Sanromán, Sci. World J. (2014).
[20] H. Zazou, N. Oturan, H. Zhang, M. Hamdani, and M.A. Oturan. Sustain Environ. Res. 27 (2017) 15.
[21] E. Brillas. J. Mex. Chem Soc. 58 (2014) 239.
[22] S. Komtchou, A. Dirany, P. Drogui, D. Robert, and P. Lafrance. Water Res. (2017).
[23] P.A. Diaw, N. Oturan, M.D.G. Seye, A. Coly, A. Tine, J.J. Aaron, and M.A. Oturan. Sep. Purif. Technol. 186 (2017) 197.
[24] N.Oturan, and M.A. Oturan. Elsevier Inc. (2018).
[25] M.A. Oturan, and J.J. Aaron. Crit. Rev. Environ. Sci. Technol. 44 (2014) 2577.
[26] G. Song, X. Du, Y. Zheng, P. Su, Y. Tang, and M. Zhou. J. Hazard Mater. 422 (2022) 126888.
[27] H. Guo, C. Zhao, H. Xu, H. Hao, Z. Yang, N. Li, and W. Xu. Environ. Res. 220 (2023).
[28] M. Gar Alalm. 7th Int. Conf. Biol. Environ. Chem. 98 (2016).
[29] O. Ganzenko, C. Trellu, N. Oturan, D. Huguenot, Y. Péchaud, E.D. van Hullebusch, and M.A. Oturan, Chemosphere 253 (2020).
[30] H. Olvera-Vargas, N. Oturan, D. Buisson, and M.A. Oturan. Chemosphere 155 (2016) 606.
[31] H. Monteil, Y. Péchaud, N. Oturan, and M.A. Oturan. Chem Eng J 376 (2019).
[32] H. Monteil, Y. Péchaud, N. Oturan, and M.A. Oturan, Chem. Eng. J (2018).
[33] O. Ganzenko, D. Huguenot, ED. van Hullebusch, G. Esposito, and M.A. Oturan, Environ. Sci. Pollut. Res. 21 (2014) 8493.
[34] I. Oller, S. Malato, and J.A. Sánchez-pérez, Sci. Total Environ. 409 (2011) 4141.
[35] H. Olvera-Vargas, C. Trellu, N. Oturan, and M.A. Oturan, Handb Environ. Chem. 61 (2018) 29.
[36] Y.Y. Lou, F. Geneste, I. Soutrel, A. Amrane, and F. Fourcade, Sep. Purif. Technol. 232 (2020).
[37] S. Polat, and P. Sayan, Adv Powder Technol. 30 (2019) 2396.
[38] E.Y. Yazici, and H. Deveci, Hydrometallurgy 139 (2013) 30.

[39] C. Dong, X. Xie, X. Wang, Y. Zhan, and Y. Yao, Food and Bioproducts Processing. 87 (2008) 139.
[40] M. Berkani, Y. Kadmi, M.K. Bouchareb, M. Bouhelassa, A. Bouzaza, Journal Pre-proofs (2020).
[41] S. Nosrati, N.S. Jayakumar, and M.A. Hashim, Desalination 266 (2011) 286.
[42] M. Cobas, MA. Sanromán, and M. Pazos. Bioresour Technol. 160 (2014) 166.
[43] H. Barabadi, S. Honary, P. Ebrahimi, A. Alizadeh, F. Naghibi, and M. Saravanan. Inorg Nano-Metal Chem 49 (2019) 33.
[44] A.M. Abioye, L.N. Abdulkadir, I.S. Sintali, M.A. Bawa, F.N. Ani, ISSAT 198 (2020) 129.
[45] K. Madi, I. Yahiaoui, F. Aissani-Benissad, C. Vial, F. Audonnet, and L. Favier, Environ. Eng. Manag. J. 18 (2019) 563.
[46] E. Pajootan, M. Arami, and M. Rahimdokht, Sep. Purif. Technol. 130 (2014) 34.
[47] Camcıoğlu, B. Özyurt, S. Şengül, and H. Hapoğlu, Desalin Water Treatment 172 (2019) 270.
[48] H. Lin, N. Oturan, J. Wu, M.A. Oturan, and H. Zhang, Handb Environ. Chem. 61 (2018) 379.
[49] M. Dolatabadi, S. Ahmadzadeh, and M.T. Ghaneian, Environ Prog Sustain Energy 39 (2020).
[50] S.Y. Guvenc, H.S. Erkan, G. Varank, M.S. Bilgili, and G.O. Engin. Water Sci. Technol. 76 (2017) 2015.
[51] M. Radwan, M. Gar Alalm, H.K. El-Etriby, J. Water Process Eng. 31 (2019) 100837.
[52] N. Bensalah, A. Bedoui, S. Chellam, and A. Abdel-Wahab, Clean-Soil, Air, Water 41 (2013) 635.
[53] Y. Wang, J. Chen, J. Gao, H. Meng, S. Chai, Y. Jian, L. Shi, Y. Wang, C. He. Sep. Purif. Technol. 272 (2021) 118884.
[54] H. Lin, N. Oturan, J. Wu, H. Zhang, and M.A. Oturan. Sep. Purif. Technol. 173 (2017) 218.
[55] M.S. Yahya, N. Beqqal, A. Guessous, M.R. Arhoutane, and K. El Kacemi. Cogent. Chem. 144 (2017) 1.
[56] MS. Yahya, M. El Karbane, N. Oturan, K. El Kacemi, and M.A. Oturan. Environ. Technol. 37 (2016) 1276.
[57] N. Oturan, M. Zhou, and M. A. Oturan, J. Phys. Chem. A 114 (2010) 10605.
[58] A. Hadj, S. Sabatino, F. Proietto, S. Ammar, A. Gadri, A. Galia, and O. Scialdone. Chemosphere 202 (2018) 111.
[59] A. Zaouak, F. Matoussi, and M. Dachraoui. J. Environ. Sci. Heal. Part B Pestic. Food Contam. Agric. Wastes 48 (2013) 878.
[60] N. Helena, L. Xiaohu, A. Nadine, C. Cátia, and A. Henrik, Chem. Eng. J. (2018).

[61] A. Ledezma Estrada, Y.Y. Li, and A.Wang. J. Hazard. Mater. 227 (2012) 41.
[62] H. Olvera-Vargas, T. Cocerva, N. Oturan, D. Buisson, and M.A. Oturan. J. Hazard. Mater. 319 (2016) 13.
[63] A. Aboudalle, F. Fourcade, AA. Assadi, L. Domergue, H. Djelal, T. Lendormi, S. Taha, A. Amrane. Chemosphere (2018).
[64] D. Mansour, and F. Fourcade, Water Air Soil Pollut. 223 (2012) 2023.
[65] C.Annabi, F. Fourcade, I. Soutrel, F. Geneste, D. Floner, N. Bellakhal, and A. Amrane, J. Environ. Manage 165 (2016) 96.
[66] E. Mousset, N. Oturan, ED Van. Hullebusch, G. Guibaud, G. Esposito, and M.A. Oturan. Water Res. 48 (2013) 306.
[67] A. Aboudalle, H. Djelal, F. Fourcade, L. Domergue, AA. Assadi, T. Lendormi, S. Taha, and A. Amrane, J. Hazard. Mater. 359 (2018) 85.
[68] B. Tak, B. Tak, Y. Kim, Y. Park, Y. Yoon, and G. Min, J. Ind. Eng. Chem. 28 (2015) 307.
[69] GK. Akkaya, HS. Erkan, E. Sekman, S. Top, H. Karaman, MS. Bilgili, and GO. Engin. Int. J. Environ. Sci. Technol. 16 (2019) 2343.
[70] E. Gilpavas, I. Dobrosz-gómez, and M.Á. Gómez-garcía. J .Water Process Eng. 24 (2018) 49.
[71] M. Moradi, F. Ghanbari, and E.M. Tabrizi, Toxicol. Environ. Chem. (2015) 37.
[72] K. Hasani, A. Peyghami, A. Moharrami, and M. Vosoughi. Arab. J. Chem. 13 (2020) 6122.
[73] M. Shoorangiz, M.R. Nikoo, M. Salari, GR. Rakhshandehroo, and M. Sadegh, Process Saf Environ. Prot. 132 (2019) 340.
[74] J. Wu, H. Zhang, N. Oturan, Y. Wang, L. Chen, and M.A. Oturan. Chemosphere 87 (2012) 614.
[75] E. Brillas, I. Sirés, and M.A. Oturan. Chem. Rev. 109 (2009) 6570.
[76] H.H. Thawini, R.H. Salman, and W.S. Abdul-Majeed. Iraqi J. Chem. Pet. Eng. 24 (2023) 13.
[77] I.A. Larralde-Pi˜na, K. Acu˜na-Askar, M. Villanueva-Rodríguez, J.L. Guzm´an-Mara, and E.J. Ruiz-Ruiz, Chemosphere (2023) 344.
[78] M. Waffo, L. Carelle, J. Marie, D. Dikdim, G.B. Noumi, and J. Marie, Biointerface Res. Appl. Chem (2023).